Variable-Energy Photoelectron Spectroscopic Studies of H_2S Chemisorption on Cu_2O and ZnO Single-Crystal Surfaces: HS^- Bonding to Copper(I) and Zinc(II) Sites Related to Catalytic Poisoning

Jianyi Lin, Jennifer A. May, Stephen V. Didziulis, and Edward I. Solomon*

Contribution from the Department of Chemistry, Stanford University, Stanford, California 94305.
Received October 22, 1991

Abstract: Adsorption of H_2S on the $Cu_2O(111)$, ZnO(0001), and ZnO(10$\bar{1}$0) surfaces has been investigated using variable-energy photoelectron spectroscopy. At room temperature, all surfaces react to form sulfide. At low temperature (140 K) and low H_2S coverages (0–0.3 L), H_2S chemisorbed on the $Cu_2O(111)$ surface is found to completely dissociate, forming sulfide and hydroxide. Under these conditions, the sulfide S 3p photoemission band is observed at 10 eV below the vacuum level, and the S $2p_{3/2}$ and $2p_{1/2}$ core levels lie at 166.4 and 167.6 eV, respectively. At intermediate coverages (0.3–3.4 L), partial deprotonation of H_2S yields HS^- on the $Cu_2O(111)$ surface, resulting in three valence band photoemission peaks at 17.0 (Cu–S–H σ), 13.8 (Cu–S pseudo-σ), and 10.3 eV (Cu–S π). At high coverages (>3.4 L), H_2S is molecularly adsorbed, producing valence band peaks at 13.9 ($1b_2$), 12.0 ($2a_1$), and 9.4 eV ($1b_1$) and S 2p core features at 168.4 ($2p_{3/2}$) and 169.6 eV ($2p_{1/2}$). Alternatively, higher H_2S exposures corresponding to an order of magnitude lower sticking probability are required for chemisorption on the ZnO surfaces at low temperature (140 K), and only coordinated HS^- is observed. Thus, the reactivity of H_2S on ZnO is fundamentally different than on Cu_2O. The valence band photoemission spectrum of this system exhibits peaks at 18.2 (Zn–S–H σ), 13.8 (Zn–S pseudo-σ), and 11.8 eV (Zn–S π), while the S 2p levels are found at 167.0 and 168.2 eV. Studies of the stabilized HS^- intermediate on the two surfaces demonstrate significant variation in their electronic structures; a greater energy splitting is observed between the M–S π and M–S pseudo-σ valence peaks for HS^- on Cu(I), indicating a stronger metal ion–SH^- bonding interaction. In addition, variable-energy PES shows the presence of more metal 4s character in the Cu(I)–SH^- σ bonding orbitals relative to the corresponding Zn(II)–SH^- levels. These results show that the bonding is stronger and reactivity is higher for H_2S on Cu(I) than on Zn(II) sites. The electronic origin of these differences in bonding and reactivity and its relation to catalytic poisoning are addressed on a molecular level.

I. Introduction

H_2S is a common source of sulfur poisoning in many catalytic processes.[1,2] In particular, Cu/ZnO catalysts for methanol synthesis and the water gas shift reaction are found to be much more sensitive to H_2S poisoning than catalysts which contain no copper component.[2-5] Studies by Auger electron spectroscopy have shown a decrease in the intensity of copper and zinc peaks with the appearance of sulfur features in the spectra of Cu-containing ZnO catalysts which were deactivated by exposure to a trace amount of H_2S, indicating that the formation of a multilayer sulfur adsorbate on the catalyst surface blocks active sites and is responsible for catalyst poisoning.[3] Studies of H_2S adsorption on surfaces relevant to methanol synthesis catalysis are therefore necessary for obtaining molecular level insight into the mechanism and increased sensitivity of the copper-promoted catalysts to sulfur poisoning.

Our previous studies of the coordination chemistry of submonolayer coverages of copper on different ZnO single-crystal surfaces and their interaction with CO have determined that a coordinatively unsaturated C_{3v} Cu(I) site appears to be the active center for high-affinity CO binding which has been correlated to high activity for methanol synthesis.[6] Although the adsorption of H_2S on metallic copper, other metals, and some semiconductor surfaces has been studied,[5,7-21] no investigation of the chemisorption of H_2S on single-crystal surfaces of zinc(II) or copper(I) oxides has been reported. This is the focus of the present investigation.

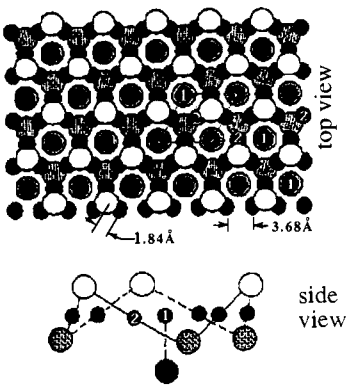

Figure 1. Structure of the ideal $Cu_2O(111)$ surface as viewed from top and side. The unit mesh of the surface lattice is indicated in the top view.

(1) Oudar, J. *Cata. Rev. Sci. Eng.* **1980**, *22*, 171.
(2) Bartholomew, C. H.; Agrawal, P. K.; Katzer, J. R. *Adv. Catal.* **1982**, *31*, 135.
(3) Gikis, B. J.; Isakson, W. E.; McCarty, J. G.; Sancier, K. M.; Schechter, S.; Wentrcek, P. R.; Wood, B. J.; Wise, H. Final Report: PERC-0060-8; SRI, 1977.
(4) Chinchen, G. C.; Denny, P. J.; Jennings, J. R.; Spencer, M. S.; Waugh, K. C. *Appl. Catal.* **1988**, *36*, 1.
(5) Campbell, C. T.; Koel, B. E. *Surf. Sci.* **1987**, *183*, 100 and references therein.
(6) Didziulis, S. V.; Butcher, K. D.; Cohen, S. L.; Solomon, E. I. *J. Am. Chem. Soc.* **1989**, *111*, 7110.
(7) Somorjai, G. A. In *Chemistry in Two Dimensions: Surfaces*; Cornell University: Ithaca, NY, 1981; p 253 and references therein.
(8) Capehart, T. W.; Seabury, C. W.; Graham, G. W.; Rhodin, T. N. *Surf. Sci.* **1982**, *120*, L441.
(9) Ling, D. T.; Miller, J. N.; Weissman, D. L.; Pianetta, P.; Stefan, P. M.; Lindau, I.; Spicer, W. E. *Surf. Sci.* **1983**, *124*, 175.
(10) Fisher, G. B. *Surf. Sci.* **1979**, *87*, 215.
(11) Moroney, L.; Rassias, S.; Roberts, M. W. *Surf. Sci.* **1981**, *105*, L249.
(12) Koestner, R. J.; Salmeron, M.; Kollin, E. B.; Gland, J. L. *Chem. Phys. Lett.* **1986**, *125*, 134; *Surf. Sci.* **1986**, *172*, 668.
(13) Kuhr, H. J.; Ranke, W. *Surf. Sci.* **1987**, *189/190*, 420.
(14) Ranke, W.; Kuhr, H. J.; Finster, J. *Surf. Sci.* **1987**, *192*, 81.
(15) Bhattacharya, A. K.; Clarke, L. J.; de la Garza, L. M. *J. Chem. Soc., Faraday Trans. 1*, **1981**, *77*, 2223.

0002-7863/92/1514-4718$03.00/0

Studies of H_2S adsorption on Zn(II) sites were performed on the ZnO(10$\bar{1}$0) and -(0001) surfaces. ZnO has a wurtzite structure which contains tetrahedral Zn(II) and oxide ions in the crystal lattice. The ZnO(10$\bar{1}$0) surface is a nonpolar face where the Zn(II) and oxide ions are arranged in coordinatively unsaturated pairs in the surface plane with a rectangular unit mesh of 3.25 × 5.21 Å, while ZnO(0001) is a polar face composed only of Zn(II) ions arranged in a hexagonal unit mesh of 3.25 Å for each unit vector (see ref 10). H_2S chemisorption of both ZnO surfaces has been studied to determine if the reactivity is dependent on these differences in surface structure. Since neither Cu/ZnO binary catalysts nor Cu-deposited ZnO single crystals are pure systems, our study of H_2S adsorption on Cu(I) sites focuses on the Cu_2O(111) single-crystal surface. Cu_2O has a high-symmetry, simple cubic structure in which each oxygen ion is surrounded by a tetrahedron of Cu ions and each copper atom is linearly coordinated to two oxygen atoms. Cu_2O(111) is a nonpolar surface with both coordinatively unsaturated oxide and cuprous ions on the topmost layer (see Figure 1). The availability of oxide ions on both the ZnO and Cu_2O surfaces is important for comparison of H_2S chemisorption on these two surfaces since oxide ions are Brønsted basic centers and can serve in the deprotonation of adsorbed H_2S. It should be noted that in these studies the HS^- group is found to exist on both Cu_2O and ZnO surfaces as a product of partial dissociative adsorption of H_2S. Since thiolate is a key ligand to Cu(I) and Zn(II) sites in sulfur-containing proteins such as metallothionine, plastocyanin, etc., these studies are also of special interest to bioinorganic chemistry.

The electronic structure of Cu_2O has been extensively studied by electron energy loss spectroscopy (EELS),[22] X-ray photoelectron spectroscopy (XPS), ultraviolet photoelectron spectroscopy (UV PES), Auger electron spectroscopy (AES), and Bremsstrahlung isochromat spectroscopy (BIS)[23] because of its optical and electric properties and recently because of the high-temperature superconducting nature of copper oxide-based materials. Most of these studies were performed on oxides grown on metal crystals, rather than single-crystal Cu_2O surfaces. Studies of the Cu_2O photoemission spectrum indicate that the valence band of Cu_2O consists of a Cu 3d band and O 2p band, which are well separated and centered at about 7 and 11 eV below the vacuum level,[24] respectively. The electronic structure of Cu_2O is quite different from that of ZnO, in which the metal 3d band is centered at 16.3 eV relative to the vacuum level, well below the O 2p level which is between 10 and 12 eV.[25,26] This difference in d^{10} electronic structure indicates that there should be differences in the interaction of Cu(I) and Zn(II) surface sites with H_2S.

In this study, we first examine the electronic structure of the clean Cu_2O(111) single-crystal surface using variable-photon-energy PES and resonant PES for comparison to our earlier data on clean ZnO.[25,26] These results are presented in section IIIA. Studies of H_2S adsorption on Cu_2O(111) are presented in section IIIB. UV PES, XPS, variable-photon-energy PES, and AES are used to investigate the adsorption-induced changes in the valence band, S 2p core levels, O 1s core level, and corresponding Auger peak regions at different H_2S coverages and temperatures. These studies find that (1) completely deprotonated H_2S dominates at room temperature as well as at very low coverages at 140 K, (2) partially deprotonated H_2S dominates at intermediate coverages at 140 K, and (3) molecularly chemisorbed H_2S dominates at high coverages at 140 K. Parallel experiments were performed for H_2S on the ZnO(0001) surface. Partially deprotonated H_2S was found for all coverages at 140 K, while completely deprotonated H_2S was found at room temperature. These results are presented in section IIIC. Based on the results and analyses in section III, differences in the reactivity of H_2S with Cu(I) and Zn(II) surface sites and HS^-–d^{10} metal ion bonding as related to catalytic poisoning are discussed in section IV.

II. Experimental Section

A Cu_2O(111) surface was prepared by cutting a 1-mm plate from a single crystal of Cu_2O, which was a gift of Dr. C. Schwab, Universite Louis Pasteur, France. The orientation of the surface was checked by Laue back diffraction (±1°), and the sample surface was polished with alumina grit down to 0.1 μm. It was then chemically etched with nitric acid, pH 1–2. Surface cleaning was completed in UHV by a series of sputter/anneal cycles. Ar sputtering was performed at energies between 250 and 300 eV at an ion flux density of 1–4 mA/cm^2; sputtering at 300–1500 eV resulted in preferential loss of oxide ions. The sample temperature was maintained at approximately 720 K throughout the sputter and anneal process. The surface cleanliness and chemical stoichiometry were monitored by AES. The oxidation state of copper was determined using the X-ray-induced Cu $L_3M_{4,5}M_{4,5}$ Auger peak. The surface order was checked by LEED, which showed a hexagonal pattern for the clean surface, indicating that no symmetry changing surface reconstruction occurs.

The ZnO sample was also a 1-mm-thick plate cut from a single crystal. The sample was oriented to within 1° of the (0001) direction by Laue backscattering, polished with alumina grit, and etched with a 5% HCl solution. Ar ion sputtering was performed at successive accelerating potentials of 1000, 500, and 250 V at 720 K in UHV, followed by annealing at this temperature. ZnO sample cleanliness was checked by AES.

All gases used were of research purity (Matheson, 99.95%). H_2S was introduced into the experimental chamber from a separate UHV line through a Varian leak valve. The H_2S pressure and exposure were monitored using an ionization gauge. The sample was heated and cooled in situ; the sample temperature was measured using a chromel–alumel thermocouple attached to the sample holder. All adsorption experiments were carried out at low temperatures. Cu_2O is a p-type semiconductor with a band gap of 2.17 eV.[27] At low temperatures, photoemission-induced charging became severe but was compensated for by using an electron flood gun (operated at 1.5–2.0 V and 2.0 A) without distorting the overall spectral shape. Any sample charging which did occur was taken into accout using the Cu 2p core and Cu 3d valence levels as references.

All experiments using resonance photon sources were carried out in a Vacuum Generators ESCALAB MK II instrument equipped with XPS, UV PES, AES, and LEED capabilities. A discharge lamp produced He II (40.8 eV) and He I (21.2 eV) photons propagating at an angle 15° off the vertical. A Mg Kα (1253.6-eV) X-ray source was used for core level studies. The base pressure of the system was maintained at ~ 5 × 10^{-11} mbar (2 × 10^{-10} mbar with the He resonance lamp in operation). The experiments employing synchrotron radiation as a photon source were performed on beam line III-1 at the Stanford Synchrotron Radiation Laboratory (SSRL) under dedicated conditions using a grasshopper monochromator. Variable inlet and exit slits on the monochromator normally maintained a constant photon energy resolution of 0.2 eV. A Perkin-Elmer PHI chamber with a double-pass cylindrical mirror analyzer (CMA), electron flood gun, and ion sputtering gun was used. The CMA accepts a 6° cone of electrons with a half-angle of 42.5° off the CMA axis. A narrow analyzer slit and a small pass energy (25 eV) were chosen for the CMA, resulting in a constant instrument resolution of 0.2 eV. Constant initial state (CIS)[28,29] spectra were obtained at the metal 3p → 4s edges. The photoelectron kinetic energy and the photon energy were simultaneously scanned through the metal 3p absorption edge. The constant initial state was set at the metal 3d satellite

(16) Beck, D. D.; White, J. M.; Ratcliffe, C. T. *J. Phys. Chem.* **1986**, *90*, 3123.
(17) Perry, D. L.; Taylor, J. A. *J. Mater. Sci. Lett.* **1986**, *5*, 384.
(18) Brundle, C. R.; Carley, A. F. *Faraday Discuss. Chem. Soc.* **1975**, *60*, 51.
(19) Hegde, R. I.; White, J. M. *J. Phys. Chem.* **1986**, *90*, 296.
(20) Joyner, R. W.; Kishi, K.; Roberts, M. W. *Proc. R. Soc. London, Ser. A* **1977**, *358*, 223.
(21) Hughes, G. J.; Humphreys, T. P.; Montgomery, V.; Williams, R. H. *Vacuum* **1981**, *31*, 539.
(22) Dubois, L. H. *Surf. Sci.* **1982**, *119*, 399.
(23) Ghijsen, J.; Tjeng, L. H.; van Elp, J.; Eskes, H.; Westerink, J.; Sawatzky, G. A.; Czyzyk, M. T. *Phys. Rev. B* **1988**, *38*, 11322.
(24) The energy levels reported here for the Cu_2O and ZnO surfaces are all referenced to the vacuum level, rather than to the Fermi level (at 4.8 eV for Cu_2O and 5.6 eV for ZnO), because at low temperatures the conductivity of Cu_2O is poor, and charging and band-bending changes can complicate the determination of the Fermi level.
(25) Gay, R. R.; Nodine, M. H.; Henrich, V. E.; Zeiger, H. J.; Solomon, E. I. *J. Am. Chem. Soc.* **1980**, *102*, 6752.
(26) Didziulis, S. V.; Cohen, S. L.; Butcher, K. D.; Solomon, E. I. *Inorg. Chem.* **1988**, *27*, 2238.
(27) Moskalenko, S. A. *Soviet Phys. Solid State* **1960**, *2*, 1587.
(28) Lindau, I.; Spicer, W. E. In *Synchrotron Radiation Research*; Winick, H., Doniach, S., Eds.; Plenum Press: New York, 1980, p 159.
(29) Kunz, C. In *Photoemission in Solids II*; Ley, L., Cardona, M., Eds.; Wiley: New York, 1978; p 299.

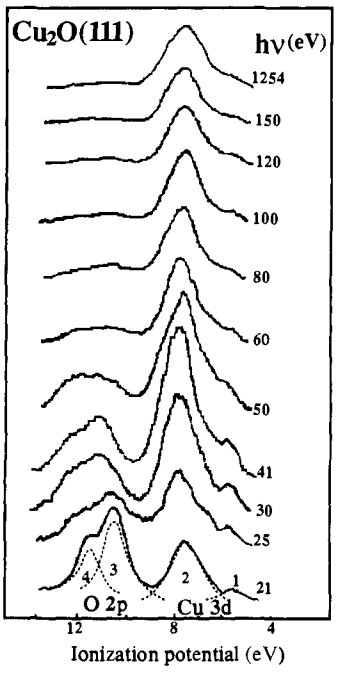

Figure 2. Variable-photon-energy PES of the clean $Cu_2O(111)$ valence band region. The spectra at all photon energies ($h\nu$) were fit with four Gaussian/Lorentzian peaks (see text).

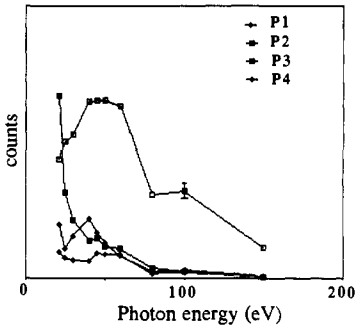

Figure 3. Photon energy dependence of the intensity of the four component peaks (P1–4) for the $Cu_2O(111)$ surface in Figure 2.

maximum. All spectra were signal-averaged until a satisfactory signal-to-noise ratio was achieved.

III. Results and Analysis

A. Clean $Cu_2O(111)$. 1. Variable-Photon-Energy PES. Variable-photon-energy photoemission spectra of the valence band region of Cu_2O are shown in Figure 2. The spectra exhibit two major bands: one at 5–9 eV and the second at 10–12 eV relative to the vacuum level. The first major band initially increases its intensity with increasing photon energy, reaching a maximum for the photon energy between 40 and 50 eV, and then decreases in intensity with higher photon energies. This delayed maximum in the photoionization cross section is characteristic of Cu 3d photoemission.[26] The second major band is intense at low photon energies, reduces its intensity dramatically with increasing photon energy, and almost vanishes at high photon energies. Based on this cross-section behavior, the band can be assigned to O 2p photoemission. Both the Cu 3d and O 2p bands are composed of two peaks. A curve-fitting procedure, which varies the position, width, and height of the four component peaks while minimizing the difference between the fit and the experimental spectra, enables one to fit the spectra at all photon energies with four Gaussian/Lorentzian peaks: peaks 1, 2, 3 and 4, at 5.5, 7.5, 10.4, and 11.7 eV, respectively. Figure 3 shows the intensity–energy profiles of the four peaks. The main part of the 3d band, peak 2, displays a delayed maximum near 45 eV, consistent with its assignment as Cu 3d photoemission. Peak 1, which has much less intensity, exhibits a different cross-section behavior from that of peak 2; it starts at relatively high intensity at low photon energies and then drops significantly before going through a maximum in the

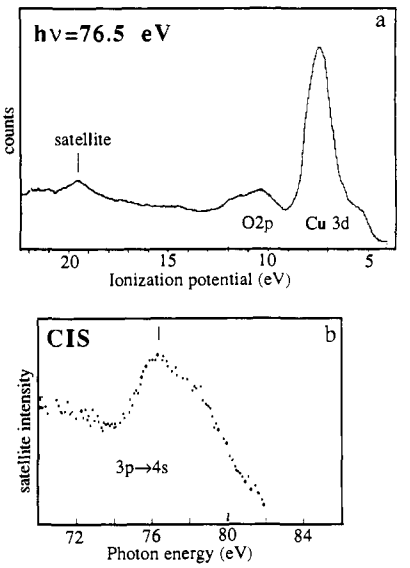

Figure 4. (a) PES of the valence band and satellite region of $Cu_2O(111)$, using synchrotron radiation of 76.5 eV. (b) Constant initial state (CIS) intensity profile of the satellite in (a) at the Cu 3p → 4s absorption edge for the clean $Cu_2O(111)$ surface. The intensity maximum is 76.3-eV photon energy and corresponds to the Cu 3p → 4s transition.

region of about 40–50 eV. This photoemission cross-section behavior indicates that there is some mixing of O 2p character into this 3d antibonding band. Peak 3 starts very intense and drops rapidly with increasing photon energy as is expected for ionization from the O 2p orbitals. Peak 4, however, exhibits differences from pure O 2p photoemission with low intensity at low photon energies and relatively high intensity near 45 eV. This cross-section behavior indicates mixing of Cu 3d character into this O 2p band. The intensity–energy profiles of the four component peaks are consistent with those expected from a tight-binding band structure calculation reported by Robertson,[30] which gives mixing coefficients for peaks 1–4 as follows: 67% Cu 3d, 23% O 2p, 10% Cu 4s for peak 1; 100% Cu 3d for peak 2; 84% O 2p, 16% Cu 4p for peak 3; and 60% O 2p, 31% Cu 3d, 9% Cu 4s for peak 4.

Parallel results for ZnO from earlier studies indicate that the Zn 3d band is composed of two peaks (peaks 1 and 2 at 16.7- and 15.9-eV ionization potential) while the O 2p band consists of three peaks (peaks 3, 4, and 5 at 12.9, 11.5- and 9.1-eV ionization potential). The mixing coefficients for these peaks are as follows: 74% Zn 3d, 26% O 2p for peak 1; 82% Zn 3d, 18% O 2p for peak 2; 85% O 2p, 5% Zn 4p, 10% Zn 4s for peak 3; 100% O 2p for peak 4; and 74% O 2p, 26% Zn 3d for peak 5.[26]

2. CIS Resonance Studies of the Cu 3p → 4s Transition. CIS experiments were performed on the Cu 3d shake-up satellite peak which appears at 19.5 eV below the vacuum level, approximately 12 eV to deeper binding energy than peak 2 of the Cu 3d band. (Figure 4a) As shown in the CIS intensity–energy profile in Figure 4b, the 3d shake-up satellite intensity is resonance-enhanced at photon energies close to 76 eV which is the Cu 3p → 4s absorption edge, while at photon energies away from resonance the satellite intensity is very weak. The mechanism of this resonance enhancement is given in Scheme I. At the Cu 3p absorption edge,

Scheme I

Cu 3p threshold excitation	$3p^63d^{10}4s^0 + h\nu \longrightarrow 3p^53d^{10}4s^1$
SCK Auger decay	$3p^53d^{10}4s^1 \longrightarrow 3p^63d^84s^1$
Cu 3d ionization plus shake-up	$3p^63d^{10}4s^0 \longrightarrow 3p^63d^84s^1$

a 3p core-level electron is excited into the Cu 4s bound state. This excited state then decays via a super Coster Kronig (SCK) Auger decay process[31] involving two d electrons. The final state produced is the same as that achieved through a 3d ionization plus 3d → 4s shake-up process which is the generally accepted model for the origin of the valence band satellite in transition-metal compounds

(30) Robertson, J. *Phys. Rev. B* **1983**, *28*, 3378.
(31) Ghosh, P. *Introduction to Photoelectron Spectroscopy*; Wiley: New York, 1983.

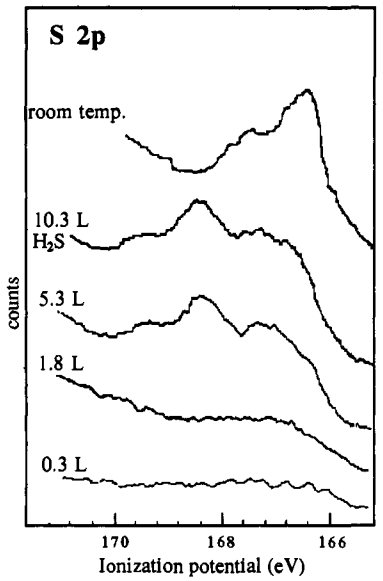

Figure 5. S 2p core level photoemission spectra for the $Cu_2O(111)$ surface exposed to 0.3, 1.8, 5.3, and 10.3 L of H_2S at 130 K and a surface which had been exposed to 10.3 L at 130 K and then warmed to room temperature. The spectra were obtained using 190-eV synchrotron radiation with the energy resolution of 0.6 eV.

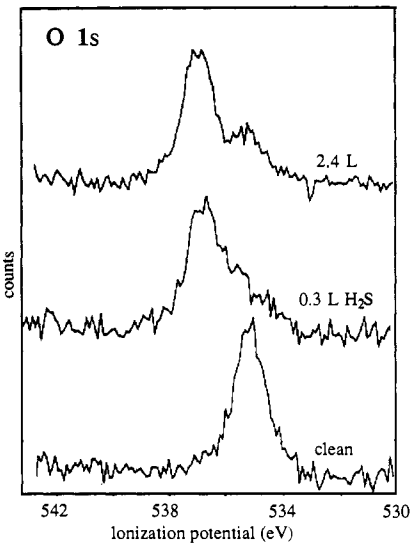

Figure 6. O 1s cove level for the $Cu_2O(111)$ surface before and after exposure to H_2S at 140 K. The spectra were taken using Mg Kα radiation with an analyzer pass energy of 20 eV which gives a 1.2-eV energy resolution.

with completely filled 3d bands.[26,32,33] Constructive interference of these two pathways results in the resonance enhancement of the 3d satellite intensity at the Cu 3p absorption edge. For Cu_2O, the Cu 3p photoemission peak lies at 79.3 eV below the vacuum level. Maximum resonance enhancement of the 3d satellite occurs at about 76.3 eV. Since the resonance arises from the 3p → 4s transition, the approximate energy of the 4s level (ignoring relaxation effects resulting from the transition to a bound state) is determined at 3 eV below the vacuum level. This value for the energy of the Cu 4s level in Cu_2O is much higher than for the Zn 4s level in ZnO (5.2 eV below the vacuum level).[26]

The final state of the Cu 3d shake-up satellite photoemission is $3p^63d^84s^1$ which has two holes in the same 3d shell. Thus, the ionization potential of the satellite, E_{sat}, is given by

$$E_{sat} = 2E_{3d} - E_{4s} + U$$

where E_{3d} and E_{4s} are the energies of the Cu 3d and Cu 4s levels and U is the effective Coulomb repulsion between two holes in the 3d subshell. From the PES data, E_{sat} = 19.5 eV, E_{3d} = 7.5 eV, and E_{4s} = 3 eV below the vacuum level (vide supra). Therefore, U = 7.5 eV for Cu_2O, which is considerably smaller than the value of 9.9 eV for ZnO.[26] The smaller value of U reflects the lower effective nuclear charge present for Cu(I), resulting in less d orbital contraction and thus less Coulomb repulsion. Further, both U values for Cu_2O and ZnO are greatly reduced from the free ion values ($U_{free\ ion}$) of 16.5 eV for Cu(I) and 19.7 eV for Zn(II).[26] This reduction is greater for Cu_2O than for ZnO, with $U_{complex}/U_{free\ ion}$ values of 0.45 for Cu_2O vs 0.50 for ZnO. Since the reduction in Coulomb repulsion of the metal ion 3d electrons reflects changes due to nephelauxetic expansion[34] of the d orbitals through covalent interactions with the ligands, the greater reduction in the U value from the free cuprous ion to Cu_2O reflects greater covalent bonding in Cu_2O than ZnO.

Thus, comparing the data on the clean Cu_2O surface with our earlier data on clean ZnO surfaces shows that the 4s energy is higher by 2.2 eV and the nephelauxetic expansion of the d orbitals is greater for Cu_2O.

B. $H_2S/Cu_2O(111)$. 1. Low Coverages (<0.3 L) at 140 K and High Coverages at Room Temperature. S 2p photoemission spectra for H_2S on Cu_2O are shown in Figure 5 and were obtained using synchrotron radiation of 190 eV, where the photoemission cross section is approximately 100 times higher than that for Mg Kα radiation, giving higher intensity and thus better energy resolution (~0.6 eV). When the $Cu_2O(111)$ surface is first saturated to 2×10^{-8} mbar of H_2S ambient at 140 K and then is warmed to room temperature, the S 2p spectrum shows two clear peaks at 166.4 and 167.6 eV (a spin–orbit splitting of 1.2 eV) (Figure 5, top spectrum). On the basis of literature data,[5,16–19,35,36] these two peaks can be assigned to the sulfide ion, S^{2-}, indicating that the surface is sulfided at room temperature. At low temperature and low coverages (starting at 0.1 L and increasing to 0.3 L exposure), the S 2p peaks are weak, broad, and in the same energy range as those for the sulfided system obtained at room temperature (Figure 5, bottom spectrum). The S 2p peaks at low coverages (<0.3 L) can then be assigned to sulfide ion, indicating complete deprotonation of H_2S dominates the initial adsorption stage at 140 K.

Figure 6 shows the O 1s spectra before and after exposing the clean surface to H_2S at 140 K. The O 1s peak of clean Cu_2O is located at 535.2 eV. After the surface was exposed to 0.3 L of H_2S, most of the O 1s intensity shifts to deeper binding energy by 1.8 eV. On the basis of data on surface OH^- groups formed on metal or oxide surfaces,[11,19,20,37–40] the new O 1s peak is attributed to the surface hydroxide group. This indicates that the protons released from the dissociative adsorption of H_2S are bound to the lattice oxide ions. Thus, the adsorption of H_2S on the $Cu_2O(111)$ surface at low coverages and low temperatures results in complete deprotonation, forming sulfide and hydroxide ions.

The background-subtracted He I UV PES spectrum for the $Cu_2O(111)$ surface exposed to 0.1 L of H_2S at 140 K is presented in Figure 7a. The spectrum of the clean surface, which is aligned and normalized to the main peak of the Cu 3d band, is also included for comparison. A large increase in intensity is observed near 10 eV. On the basis of the data reported for cuprous and other sulfides,[8,9,35] this feature can be assigned to the S 3p levels for the S^{2-} species. This assignment is supported by the He I photoemission spectrum of the sulfided surface obtained at room

(32) Thuler, M. R.; Benbow, R. L.; Hurych, Z. *Phys. Rev. B* **1982**, *26*, 669.
(33) Ishii, T.; Taniguchi, M.; Kakizaki, A.; Naito, K.; Sugawara, H.; Nagakura, I. *Phys. Rev. B* **1986**, *33*, 5664.
(34) Jørgensen, C. K. *Oxidation Numbers and Oxidation states*; Springer: New York, 1969; p 89.
(35) Domashevskaya, E. P.; Terekhov, V. A.; Marshakova, L. N.; Ugai, Ya. A.; Nefedov, V. I.; Sergushin, N. P. *J. Electron Spectr. Relat. Phenom.* **1976**, *9*, 261.
(36) Wagner, C. D.; Riggs, W. M.; Davis, L. E.; Moulder, J. F.; Mullenberg, G. E. *Handbook of X-ray Photoemission Spectroscopy*, 2nd ed.; Perkin-Elmer: New York, 1979; p 28.
(37) Fisher, G. B.; Sexton, B. A. *Phys. Rev. Lett.* **1980**, *44*, 683.
(38) Tobin, J.; Hirschwald, W.; Cunningham, J. *Spectrochim. Acta B* **1985**, *40*, 725.
(39) McIntyre, N. S.; Rummery, T. E.; Cook, M. G.; Owen, D. *J. Electrochem. Soc.* **1976**, *123*, 1164.
(40) Barteau, M. A.; Madix, R. J. *Surf. Sci.* **1984**, *140*, 108.

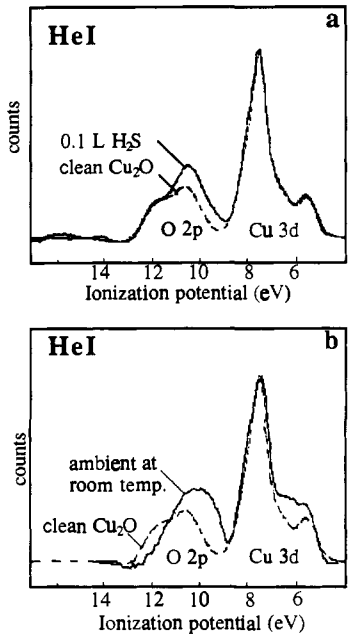

Figure 7. (a) Background-subtracted He I UV PES of the $Cu_2O(111)$ surface exposed to 0.1 L of H_2S at 140 K. (b) HeI UV PES of a $Cu_2O(111)$ surface which was exposed to 2×10^{-8} mbar of ambient H_2S at 140 K and then warmed to room temperature. For both a and b, the clean surface spectrum is included, aligned, and normalized to the Cu 3d band.

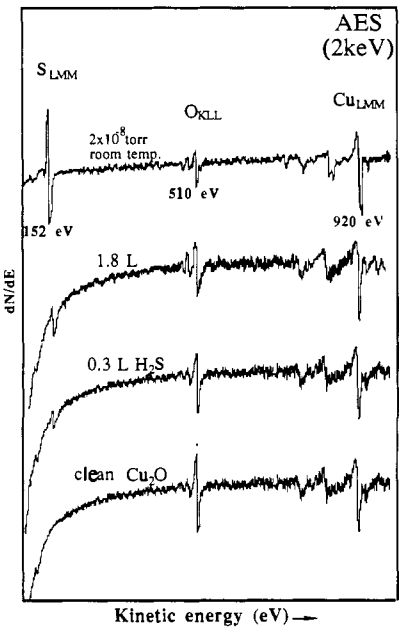

Figure 8. Auger spectra for H_2S exposures of 0, 0.3, and 1.8 L on $Cu_2O(111)$ at low temperature and at 2×10^{-8} Torr of H_2S ambient at room temperature (top). The spectra are normalized to the Cu_{LMM} signal to compare changes in the O_{KLL} and S_{LMM} signals. A primary beam energy of 2 keV was used, which limits the electron (or heat) induced desorption of molecularly adsorbed H_2S.

temperature. When the $Cu_2O(111)$ surface which is saturated to 2×10^{-8} mbar of H_2S ambient at 140 K is warmed to room temperature, the He I spectrum (Figure 7b) shows a pronounced increase in intensity at approximately 10 eV and a decrease in intensity at approximately 12 eV. The increase in intensity at 10 eV parallels the low-temperature, low-coverage data in Figure 7a, demonstrating that a large portion of the oxide ions on the surface has been replaced by S^{2-} ions. The decrease in intensity at 12 eV in Figure 7b indicates the loss of surface oxide ions due to the surface reaction at room temperature. The surface reaction also induces changes in the Cu 3d band, resulting in some intensity enhancement near 6 eV.

The AES data in Figure 8 shows that the intensity ratio of the O_{KLL} signal vs Cu_{LMM} decreases with increasing S_{LMM} intensity, indicating that surface oxide is lost with increasing H_2S exposure. This becomes most evident when the sulfur-covered surface is warmed to room temperature (Figure 8, top spectrum). The loss of surface oxide ions is consistent with the formation and desorption of water as a result of H_2S deprotonation.

2. Intermediate Coverages (0.3–3.4 L) at 140 K. When the $Cu_2O(111)$ surface is maintained at 140 K and the H_2S exposure dose is increased (from 0.3 to 3.4 L), the intensity of the S 2p peak increases with increasing H_2S exposure. The increased intensity is primarily distributed at higher binding energy relative to the low coverage spectrum (Figure 5) and represents additional contributions from protonated sulfur species. In the valence band spectrum, two peaks, A and B, appear at 17.0 and 13.8 eV (Figure 9). These two peaks rise together with increasing exposure and reach a maximum in intensity at an exposure of approximately 3.4 L. Since the intensity changes of peaks A and B are parallel, they are attributed to the same adspecies. Based on the gaseous H_2S photoemission spectrum which has three highest energy occupied molecular orbitals (i.e., $1b_1$, $2a_1$, and $1b_2$) at 10.3 13.2, and 15.1 eV, respectively,[41] the energy positions of peaks A and B are too deep to be assigned to molecularly adsorbed H_2S. Nor can these two peaks be ascribed to the S 3s-derived orbital which would appear near 22 eV.[41] Thus, they are assigned to a surface-bound HS^- group, produced by the partial deprotonation of H_2S. This assignment is consistent with self-consistent field–$X\alpha$–scattered wave (SCF–$X\alpha$–SW) calculations[42] as discussed in section IV. In addition to peaks A and B, peak C, which overlaps the oxide band, increases in intensity up to an exposure of 3.4 L, indicating that this is likely a third peak associated with HS^-. These changes are more evident when synchrotron radiation is used because of the higher photoionization cross section of S 3p at low photon energies.[43]

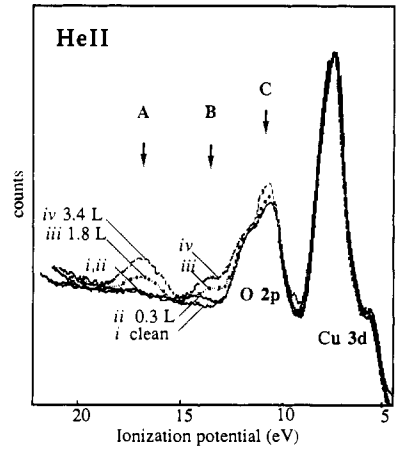

Figure 9. He II ultraviolet photoelectron spectra of $H_2S/Cu_2O(111)$ system with increasing coverages (0.3–3.4 L) at 140 K. The spectra are aligned and normalized to the Cu 3d main peak. The adsorption-induced features are labeled as A, B, and C, the latter being superimposed on the substrate oxide band.

Photoemission spectra of the valence band region of the $H_2S/Cu_2O(111)$ system at 1.8 L and 130 K have been recorded from 25 to 120 eV photon energy and are presented in Figure 10. The clean surface spectrum at each photon energy is also included for comparison. From Figure 9, the surface HS^- group is the dominant adspecies at this coverage, exhibiting three peaks, A,

(41) Siegbahn, K.; Nordling, C.; Johansson, G.; Hedman, J.; Heden, P. F.; Hamrin, K.; Gelius, U.; Bergmark, T.; Werme, L. O.; Manne, R.; Baer, Y. *ESCA Applied to Free Molecules*; North-Holland: Amsterdam, 1969; p 87.

(42) Penfield, K. W.; Gerwirth, A. A.; Solomon, E. I. *J. Am. Chem. Soc.* **1985**, *107*, 4519.

(43) Yeh, J. J.; Lindau, I. *At. Data Nucl. Data Tables* **1985**, *32*, 1.

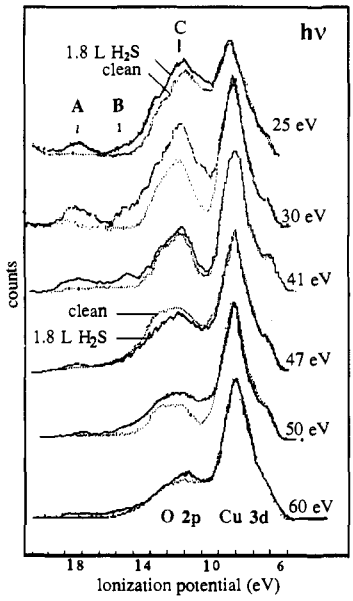

Figure 10. Photon energy dependence of the valence band spectra for the HS^--covered (1.8 L of H_2S exposure at 130 K) (solid line) and clean $Cu_2O(111)$ surfaces (dashed line). In each set of spectra, clean data are normalized and aligned to the Cu 3d band. The adsorption-induced features are labeled as peaks A, B, and C.

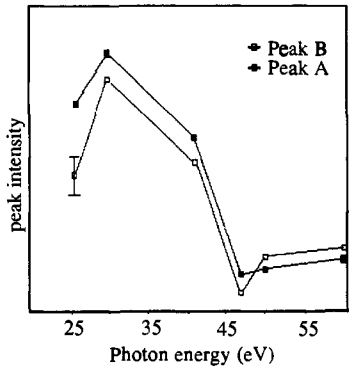

Figure 11. Intensity–energy profiles of peaks A and B in the $H_2S/Cu_2O(111)$ spectrum in Figure 9. The perceived minimum at 47 eV is not outside the error bars of the measurement.

B, and C, in the photoemission spectrum. Figure 10 shows a significant and similar dependence of the intensity of peaks A and B on photon energy. These peak intensities are plotted as a function of photon energy in Figure 11. Peak C also shows a similar intensity vs photon-energy behavior but is complicated due to overlap with the substrate oxide region. At low photon energies, the peak intensities increase with increasing photon energy and show a maximum at 30 eV. They then decrease with further increase in photon energy. The large intensity increase to lower photon energies in the intensity–energy profile demonstrates that peaks A and B (and C) are mainly of S 3p character, consistent with their assignment as photoemission from a surface-bound HS^- species. Further, the occurrence of a decrease in intensity below 30 eV in Figure 11 is characteristic of Cu 4s photoemission (due to its cooper minimum at ~16-eV photon energy).[43] Thus, Cu 4s character is mixed into the molecular orbitals of the surface HS^- group via Cu–SH^- bonding. Since the interaction of the HS^- ligand with the filled 3d levels will not contribute to net bonding of HS^- to the Cu(I) surface site, the interaction with the unoccupied Cu 4s (and 4p) levels is of particular importance to bonding. The nature of this bonding and the assignment of the HS^- peaks will be discussed in section IV.

3. High Coverages (>3.4 L) at 140 K. At high coverages (5.3 and 10.3 L in Figure 5), the S 2p peak intensity continues to increase, and two peaks clearly develop at 168.4 and 169.6 eV (the energy splitting of 1.2 eV corresponding to the spin–orbit

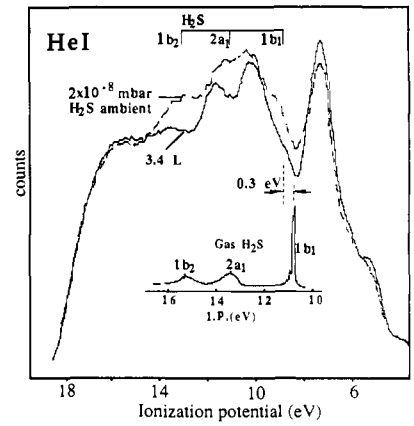

Figure 12. He I UV PES of the $H_2S/Cu_2O(111)$ system at high coverages at 140 K. The solid line is for the surface exposed to 3.4 L of H_2S, while the broken line is for the surface maintained in 2×10^{-8} mbar of ambient H_2S. The gas-phase spectrum of H_2S (obtained from: Rabalais, J. W. *Principles of UPS*; Wiley-Interscience: New York, 1977; p 161) is also included and aligned to peak $1b_2$ for comparison. This alignment requires an extramolecular relaxation shift of the H_2S gas-phase spectrum to lower binding energy by 2.1 eV.

splitting of the S 2p levels). The energies of these two peaks are analogous to those reported for adsorbed molecular H_2S.[18,19] Therefore, the new adspecies dominating at high coverage at low temperatures can be identified as molecularly adsorbed H_2S.

Figure 12 gives two He I photoemission spectra of the H_2S/Cu_2O surface, one at an exposure of 3.4 L and the other at equilibrium with 2×10^{-8} mbar of ambient H_2S (>50 L). It is clear that at high coverages new features appear at 13.0, 11.1, and 8.5 eV. These features reach a maximum in intensity at 2×10^{-8} mbar of ambient H_2S and diminish if this H_2S-saturated overlayer is irradiated by a 2-keV electron beam which is used for the AES measurement. There is a strong similarity between these energy splittings and those of the three highest occupied orbitals of gaseous H_2S ($1b_2$, $2a_1$, and $1b_1$, inserted in Figure 12), consistent with the assignment of this species as molecularly chemisorbed H_2S. In comparison with gaseous H_2S, these peaks are shifted to lower ionization potential by 2.1 eV due to extramolecular relaxation. After relaxation, a shift to deeper ionization energy of only 0.3 eV is observed for the $1b_1$ highest occupied molecular orbital upon chemisorption. This indicates that the bonding between molecular H_2S and the surface is weak, in agreement with the facile desorption induced by the AES electron beam.

C. $H_2S/ZnO(0001)$ and -$(10\bar{1}0)$. The electronic structure of the clean ZnO surface has been previously studied using variable-energy and resonant PES.[25,26] The adsorption of H_2S on the ZnO(0001) and -$(10\bar{1}0)$ surfaces is less complicated than on the $Cu_2O(111)$ surface. The reactivity of both surfaces is found to be very similar so only the data for ZnO(0001) are presented. Figure 13 gives S 2p photoemission spectra for the H_2S/ZnO-(0001) system obtained with both synchrotron radiation of 190 eV and Mg Kα radiation. No S 2p signal can be observed until the H_2S exposure dose is increased to 0.3 L. With increasing H_2S exposure up to 5.0 L, S 2p peaks grow in intensity but remain at the same energy position, 167.0 and 168.2 eV below the vacuum level (Figure 13), indicating that there is only one sulfur-containing adspecies present on the ZnO surfaces at low temperatures. No additional peaks appear even when the surface is maintained in 2×10^{-8} mbar of H_2S ambient. When the H_2S-covered surface is warmed to room temperature, the S 2p peaks are shifted to lower ionization potential by 1.0 eV and are found at 166.0 and 167.2 eV (Figure 13, top). For the H_2S/Cu_2O surface in Figure 5, we find peaks at 168.4 and 169.6 eV for molecular H_2S and 166.4 and 167.6 eV for sulfide ion, respectively, giving a 2-eV energy shift between molecular H_2S and its completely deprotonated product. Accordingly, for the H_2S/ZnO surface, we can assign the S 2p peaks at 166.0 and 167.2 eV which are observed for the H_2S-covered surface at room temperature to the sulfide ion; the

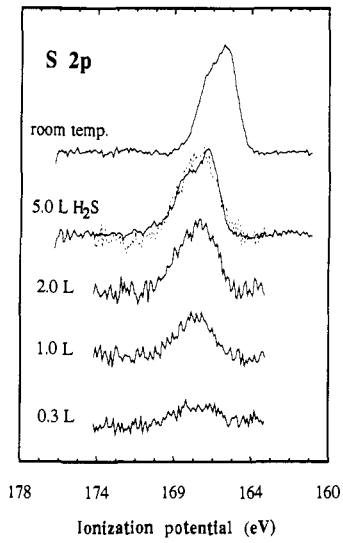

Figure 13. S 2p core level photoemission spectra of ZnO(0001) at 140 K exposed to 0.3, 1.0, 2.0, and 5.0 L of H_2S (dashed) taken with Mg Kα radiation and at 130 K exposed to 5.0 L of H_2S (solid) taken with synchrotron radiation at 190 eV. The top spectrum, taken with synchrotron radiation, corresponds to a surface which is exposed to 7.5 L at 130 K and warmed to room temperature. To compensate for cross-sectional and flux differences due to the two sources, spectra were scaled to the 5.0-L exposure data.

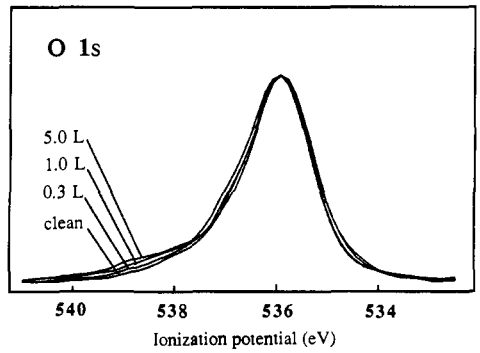

Figure 14. O 1s cove level XPS for the ZnO(0001) surface exposed to 0.3, 1.0, and 5.0 L of H_2S at 140 K. The clean surface spectrum is included normalized to the main peak. The spectra were taken using Mg Kα radiation with an analyzer pass energy of 20 eV which corresponds to an energy resolution of 1.2 eV.

S 2p peaks at 167.0 and 168.2 eV at low temperature would correspond to a surface HS^- group, based on the 1-eV energy difference between this species and the sulfide ion.

The minimum H_2S exposure at which the S 2p signal becomes observable is 0.3 L on ZnO(0001) and 0.1 L on Cu_2O(111). On the basis of the sizes of the unit mesh of the ZnO(0001) and Cu_2O(111) surfaces, the metal ion density for the ZnO(0001) surface should be approximately 4 times larger than that for the Cu_2O(111) surface. Therefore, the initial sticking probability is at least 10 times smaller for H_2S/ZnO(0001) than for H_2S/Cu_2O(111). The sticking probability is dependent on surface coverage. At an exposure of 5 L of H_2S, the intensity ratio of S 2p vs Zn 3d is approximately equal to that of S 2p vs Cu 3d for the Cu_2O surface exposed to 1.8 L of H_2S.[44] This indicates that the sticking probability for H_2S/ZnO at higher coverages is ~3 times smaller than for H_2S/Cu_2O.

Figure 14 presents O 1s X-ray photoemission spectra for the H_2S/ZnO(0001) surface as a function of H_2S coverage. The O 1s peak of the clean surface, which is at 535.9 eV, is included for comparison, aligned, and normalized to the main peak. Exposing

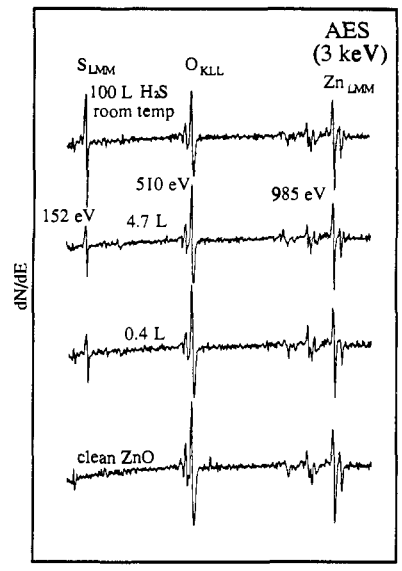

Figure 15. Auger electron spectra for the ZnO(0001) surface for 0, 0.4, and 4.7 L of H_2S at 140 K and 100 L at room temperature. The energy of the primary electron beam is 3 keV. The spectra are normalized to the Cu_{LMM} signal to compare changes in the O_{KLL} and S_{LMM} signals.

the surface to H_2S results in an increase in the intensity at 1.8 eV deeper binding. The adsorption-induced O 1s feature is attributed to the surface hydroxide group, based on the analysis of the Cu_2O data in section IIIB. The adsorption-induced O 1s feature grows with increasing exposure and becomes strongest (~15% of main peak) at the 5.0 L exposure. Further increasing the H_2S exposure has little effect on the O 1s spectrum. Combined with the S 2p XPS data, the O 1s core level data indicate that partial dissociative adsorption of H_2S occurs at low temperature (140 K), forming HS^- and surface hydroxide.

In contrast to the O 1s data in Figure 6 for the H_2S/Cu_2O system which shows almost complete protonation of surface oxide, the conversion ratio (i.e., the hydroxide to oxide O 1s ratio) is smaller for the H_2S/ZnO(0001) system in Figure 14. This can be understood in terms of the reaction stoichiometries, surface structure, and loss of water for Cu_2O (vide supra). The metal to oxygen ratio is 1:1 for ZnO compared to 2:1 for Cu_2O. Each adsorbed H_2S would produce one proton (due to partial deprotonation) on ZnO while producing two protons (due to complete deprotonation) on Cu_2O. Therefore, the conversion ratio on Cu_2O(111) should be ~4 times larger than on ZnO(0001). Additionally, the van der Waals diameter of a sulfur atom is 3.7 Å,[45] which is greater than the smallest Zn–Zn distance of 3.25 Å in ZnO(0001). The diameter of the SH^- group is expected to be even larger. Consequently, on ZnO(0001) less than half of the total number of the surface metal sites should interact with H_2S. Compared to the H_2S/Cu_2O system, the O 1s signal attributed to the surface hydroxide in the H_2S/ZnO system grows in parallel with the S 2p core feature as the exposure is increased. Also, from the Auger spectra for H_2S/ZnO(0001) in Figure 15, little O_{KLL} signal is lost with increasing H_2S exposure until the surface is sulfided. These data indicate that formation and desorption of water at low temperatures is significantly greater on Cu_2O (111).

He II UV PES spectra exhibit intensity increases at 18.2, 13.8, and 11.8 eV (labeled as L, M, and N in Figure 16), when the ZnO(0001) surface is maintained at 140 K and exposed to increasing H_2S. Further increase of the H_2S exposure above 5.0 L results in little additional change. Based on peak energy positions which are similar to those of the H_2S/Cu_2O system at intermediate coverages (Figure 9), peaks L, M, and N can be attributed to the surface HS^- group, in agreement with the above

(44) Based on the valence band data obtained using synchrotron radiation as the photon source, the intensity of Zn 3d is approximately 4 times as strong as that of Cu 3d, in agreement with the metal ion density ratio calculated from the surface structural models.

(45) Weast, R. C.; Lide, D. R.; Astle, M. J.; Beyer, W. H. *Handbook of Chemistry & Physic, 70th* ed.; CRC Press: Boca Raton, FL, 1990; p D190.

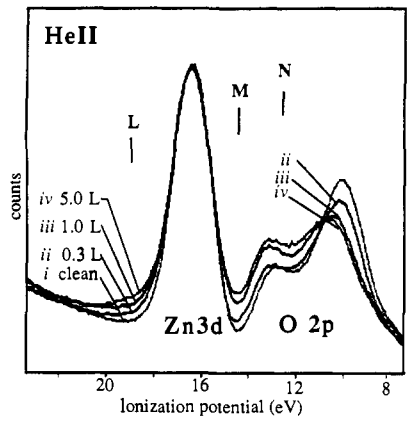

Figure 16. He II ultraviolet photoelectron spectra of the H_2S/ZnO-(0001) system with increasing H_2S coverage at 140 K. The spectra are aligned and normalized to the Zn 3d main peak. The adsorption-induced peaks at 18.2, 13.8, and 11.8 eV below the vacuum level are labeled L, M, and N, respectively.

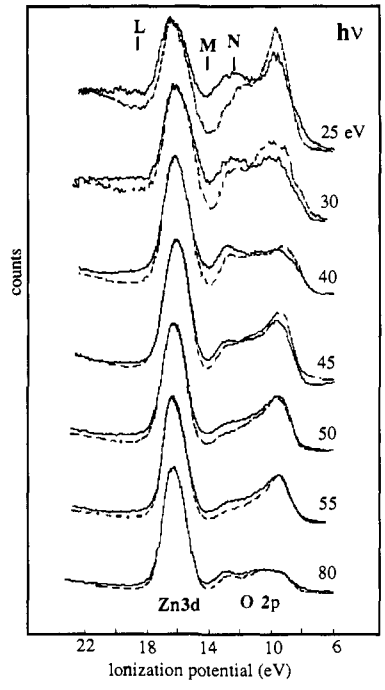

Figure 17. Photon energy dependence of the valence band spectra of the HS^--covered (7.5 L of H_2S exposure at 130 K) (solid line) and clean ZnO(0001) surfaces (dashed line). In each set of spectra, clean data are normalized and aligned to the Zn 3d band.

XPS S 2p core level results. In contrast to the H_2S/Cu_2O system, no molecularly adsorbed H_2S is found by UV PES at high exposures even when the surface is maintained in 2×10^{-8} mbar of ambient H_2S at 140 K, indicating that no available surface sites remain and that the temperature is not low enough for physisorption. When the surface is warmed to room temperature, the adsorption-induced features diminish, and the oxide band is attenuated due to sulfide formation (i.e., the lower cross section of S 3p relative to O 2p at He II photon energy).

The energy dependence ($h\nu$ = 25–120 eV) of valence-band PES peaks of the chemisorbed HS^- species (7.5 L of H_2S exposure) at 130 K is presented in Figure 17. The clean surface spectrum at each photon energy is also included for comparison. Figure 17 shows that the intensities of peaks L, M, and N are quite dependent on photon energy. The peak intensities of L and M, which were obtained from the H_2S-covered minus clean difference spectra, are plotted as a function of photon energy in Figure 18 (peak N is complicated due to overlap with the substrate oxide region). Both peaks L and M start relatively intense at low photon energy and drop rapidly with increasing photon energy as expected

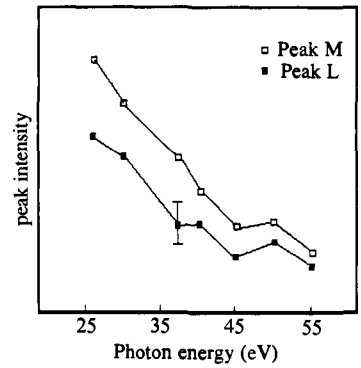

Figure 18. Intensity–energy profiles of peaks L and M in the H_2S/ZnO(0001) spectrum in Figure 17.

for ionization from the S 3p orbitals.[43] In contrast to the $H_2S/Cu_2O(111)$ system in Figure 11, the intensity does not decrease at photon energies below 30 eV. Thus, there is no evidence for a Zn 4s contribution to the HS^-–metal ion bonding.

IV. Discussion

The adsorption of H_2S on the $Cu_2O(111)$ surface at 140 K proceeds in three stages. Complete dissociative adsorption starts at low H_2S exposures (beginning at 0.1 L, which is our lowest limit of detectability, and increasing to 0.3 L), resulting in the formation of sulfide which is observed from the S 3p valence band at 10 eV in the He I photoemission spectrum (Figure 7) and the $2p_{3/2}$ and $2p_{1/2}$ peaks at 166.4 and 167.6 eV in the S 2p core level PES data (Figure 5). The protons released from the deprotonation form surface hydroxide groups as shown by the presence of the O 1s peak at 537.0 eV, 1.8 eV to deeper ionization potential relative to the clean oxide O 1s level (535.2 eV) (Figure 6). At intermediate coverages (0.3–3.4 L), the surface HS^- group dominates, producing PES peaks at 17.0, 13.8, and 10.3 eV in the valence band region (Figure 9). At high coverages, H_2S is molecularly adsorbed as indicated by the presence of peaks at 13.9, 12.0, and 9.4 eV in the He I photoemission spectrum (Figure 12) and by S $2p_{3/2}$ and $2p_{1/2}$ peaks at 168.4 and 169.6 eV (Figure 5).

Complete deprotonation of H_2S to yield sulfide is not found to occur on the ZnO(0001) surface at low temperature but occurs only at room temperature, as indicated by the S 2p peaks at 166.0 and 167.2 eV in Figure 13. At low temperatures, the sticking probability of H_2S on ZnO is estimated to be approximately 10 times smaller than on Cu_2O at the initial adsorption stage and 3 times smaller at higher coverages. Only one sulfur-containing adspecies, the surface HS^- group, is found on ZnO at all coverages, based on the presence of peaks at 18.2, 13.8, and 11.8 eV (L, M, and N in Figure 16) in the He II photoemission spectrum and on the appearance of the S $2p_{3/2}$ and $2p_{1/2}$ peaks at 167.0 and 168.2 eV in the core level PES spectrum (Figure 13). No spectroscopic feature corresponding to molecularly adsorbed H_2S is evident even at high exposures at low temperatures.

The results summarized above indicate a smaller sticking probability and reduced effectiveness in rupturing an S–H bond for ZnO as compared to Cu_2O, implying that the reactivity of H_2S on ZnO single crystal surfaces at low temperatures is much reduced from that on $Cu_2O(111)$. This is parallel to the known catalytic chemistry where copper-promoted ZnO catalysts are much more sensitive to sulfur poisoning than are ZnO catalysts containing no copper component.[3]

Under controlled conditions (~140 K and low H_2S coverages), complete dissociation occurs on the $Cu_2O(111)$ surface but not on the ZnO(0001) surface. This complete deprotonation is dependent on the availability of multiple empty oxide sites on the $Cu_2O(111)$ surface: initially the adsorbed H_2S decomposes completely; at intermediate coverages the dissociation is limited by the decrease in the number of open oxide sites producing surface HS^- groups, while at high coverages nondissociative adsorption mainly occurs. Complete dissociation of H_2S occurs at 170–180 K for W(100),[15] 185 K for Pt(111),[12] and 370 K for Pb[20] and does

not occur on many semiconductor surfaces, including Si(111),[48] Ge(111),[13] GaAs(110),[14] and InP(110)[21] even at room temperature. The effectiveness of $Cu_2O(111)$ in the decomposition of H_2S partially derives from the involvement of the surface oxide ions, which serve as Brønsted basic sites and bind protons with high affinity (i.e., high pK_a).[46] The basicity of an oxide is closely related to the value of its O 1s binding energy.[47] From Figures 6 and 14, similar values of the O 1s binding energy are observed for clean ZnO and Cu_2O surfaces (535.9 vs 535.2 eV). These values would classify the oxide ions of the ZnO and Cu_2O surfaces both as having strong basic character.[47] The reduced reactivity of the ZnO surfaces with respect to complete deprotonation of H_2S is therefore not due to reduced basicity. The reduced reactivity of the ZnO surfaces (including the $ZnO(10\bar{1}0)$ surface which contains coordinatively unsaturated surface oxide ions) must then be related to a weaker bonding interaction between the hydrogen sulfide derived species and the Zn(II) as compared to the Cu(I) surface sites.

At room temperature, bulk thermodynamics show that the reactions of both Cu_2O and ZnO with H_2S to form the metal sulfide and water have negative free-energy changes and should be spontaneous.[49] Specifically, the ΔG^{298} for the reaction $Cu_2O(s) + H_2S(g) \rightarrow Cu_2S(s) + H_2O(g)$ is −33 kcal/mol and ΔG^{298} = −19 kcal/mol for the ZnO to ZnS reaction.[50] It should be noted that the driving force of the metal oxide to sulfide reaction is the formation of water as both metal oxides are significantly more stable than their respective sulfides. The more negative ΔG for the cuprous sulfide formation is consistent with a greater Cu_2O room-temperature reactivity and indicates greater stability of the Cu(I)–S bond relative to the Cu(I)–O bond than exists in the Zn(II) species.

Our study of NH_3 adsorption on ZnO and CuCl (which contains coordinatively unsaturated C_{3v} Cu(I) sites) surfaces indicates that the bonding between NH_3 (which is a σ-donor molecule with a large dipole moment of 1.47 D) and metal ions has contributions from both σ-type covalent and electrostatic interactions, with the former being stronger in the NH_3/CuCl system and the latter stronger in the NH_3/ZnO system.[51] The electrostatic interaction would also be stronger for the H_2S-derived adspecies on Zn(II) surface sites because of the larger effective nuclear charge of Zn(II) relative to Cu(I) surface sites (~1.0 vs 0.5).[51] Therefore, the stronger interaction of H_2S-derived species with Cu_2O mainly derives from a stronger covalent bonding interaction with the metal ion surface site.

In order to compare the covalent bonding interaction of H_2S-derived species to Zn(II) vs Cu(I) sites, we focus on the surface-bound HS^- group which is the common adspecies obtained on both surfaces at 140 K. The surface-bound HS^- group is found on the ZnO surface at all levels of H_2S exposure at 140 K and is a stabilized adspecies on the $Cu_2O(111)$ surface due to the reduction in the number of nonprotonated oxide sites present in the intermediate coverage region.

The photoemission peaks corresponding to the three highest energy occupied molecular orbitals of the surface HS^- ligand are found to be at 17.0, 13.8, and 10.3 eV (peaks A, B, and C in Figure 9) for Cu(I) and at 18.2, 13.8, and 11.8 eV (L, M, and N in Figure 16) for Zn(II), respectively. On the basis of our previous $X\alpha$ calculations on thiolate binding to copper sites,[42] these three peaks can be assigned to the M–S–H σ-bonding level, M–S pseudo-σ-bonding level, and M–S π level in order of decreasing binding energy. The M–S π levels and the M–S pseudo-σ-bonding level derive primarily from the doubly degenerate π orbitals of the free HS^- ligand, which have mostly sulfur 3p character and split into two nondegenerate levels upon coordination to a metal ion (see Figure 19 which reasonably assumes a M–S–H angle of less than 180°). The M–S π level is the out-of-plane (H–S–M) component which forms a π bond between the metal ion and sulfur. The M–S pseudo-σ-bonding level is an in-plane component with electron density primarily localized along the M–S axis. It is stabilized and mixed considerably with the S–H σ orbital. The M–S–H σ-bonding level is a σ molecular orbital significantly delocalized over the M–S–H bond.

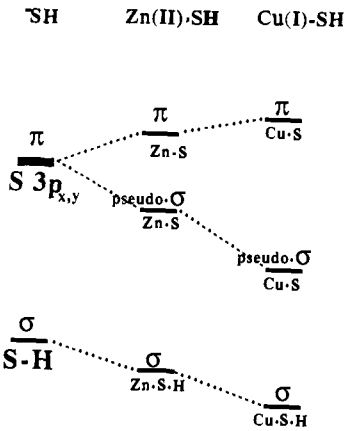

Figure 19. Interaction of the highest energy valence S 3p (π and σ) orbitals of the free HS^- ligand with Cu(I) and Zn(II) d^{10} metal ions. Upon coordination, the degenerate π orbitals, which mainly involve the S 3p lone pair electrons in the free HS^- ligand, are split into two nondegenerate levels. The first is the out-of-plane (H–S–M) component, which forms a π bond with metal ion. The second is in-plane component, stabilized due to σ bonding with the metal ion. The orbital at deepest binding energy is a σ orbital delocalized over the M–S–H bond.

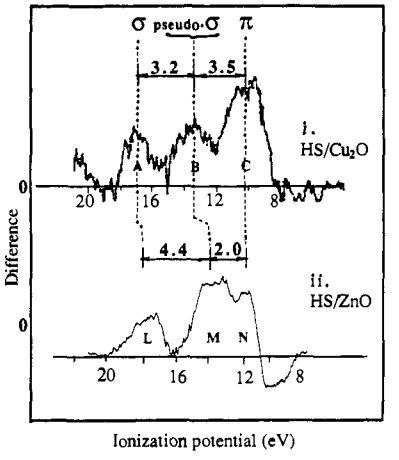

Figure 20. Comparison of the difference spectra assigned to the surface HS^- species on the $Cu_2O(111)$ and ZnO(0001) surfaces. Difference spectrum i is obtained by subtracting the clean $Cu_2O(111)$ surface spectrum from the spectrum of the H_2S (1.8 L)/$Cu_2O(111)$ system at 130 K; ii is the H_2S (5 L, 140 K)/ZnO(0001) minus clean ZnO(0001) difference spectrum. Difference spectra are aligned to the M–S π level (peak C in i and peak N in ii) for comparison, which corresponds to a shift of 1.5 eV to lower binding energy of the HS^-/Zn(II) system.

From variable-photon-energy PES studies, we find significant metal 4s character in the intensity–energy profile in the Cu(I)–SH^- system (see Figure 11) but no measurable 4s mixing in the Zn(II)–SH^- system (Figure 18), indicating a stronger covalent bonding interaction for Cu(I)–SH. This is supported by the quantitative energy splittings of the three HS^- peaks for the two surfaces. Figure 20 presents difference spectra (covered minus clean) for HS^- binding to Cu(I) vs Zn(II). The two spectra are aligned to the M–S π level (the least bonding) for comparison. Note that the B–C splitting increases relative to the M–N splitting

(46) Huheey, J. E. *Inorganic Chemistry*, 2nd ed.; Harper and Row: New York, 1978.
(47) Vinek, H.; Noller, H.; Ebel, M.; Schwarz, K. *J. Chem. Soc., Faraday Trans. 1*, **1976**, *73*, 734.
(48) Fujiwara, K. J. *J. Chem. Phys.* **1981**, *75*, 5172.
(49) Wagman, D. D.; Evans, W. H.; Parker, V. B.; Schumm, R. H.; Halow, I.; Bailey, S. M.; Churney, K. L.; Nuttall, R. L. *J. Phys. Chem. Ref. Data 11*, **1982**, Suppl. 2.
(50) No $\Delta G_f°$ was available in ref 49 for the wurzite form of ZnS, requiring the use of $\Delta G_f°$ for the sphalerite form. On the basis of the ΔH for the wurzite form, its $\Delta G_f°$ should be approximately 2 kcal/mol less negative, lowering the ΔG for the reaction.
(51) Lin, J.; Jones, P. M.; Lowery, M. D.; Gay, R. R.; Cohen, S. L.; Solomon, E. I. *Inorg. Chem.*, in press.

and the A–B splitting decreases relative to the L–M splitting. From Figure 19, a stronger bonding interaction should result in larger energy stabilizations of the two deeper energy σ-type orbitals relative to the S $3p_\pi$ orbital, the pseudo-σ being the more stabilized. A weaker metal–sulfur covalent bonding interaction for Zn(II)–SH^- over Cu(I)–SH^- is as expected from Pearson's hard and soft acid–base model which classifies Cu(I) as a soft acid, Zn(II) as borderline, and HS^- ligand as a soft base,[46] the soft acid site interacting more strongly with the soft base.

From an electronic structure point of view, both Zn(II) and Cu(I) have fully occupied 3d orbitals which cannot contribute to HS^-–metal ion bonding with ligand orbitals which are also fully occupied. Net bonding mainly derives from the interaction between the ligand orbitals, $\phi_{S_{3p}}$, and the unoccupied metal 4s (and 4p) levels, $\phi_{M_{4s}}$. The energy of bonding, $\Delta E_{M_{4s},S_{3p}}$, depends on the resonance matrix element $H_{M_{4s},S_{3p}} = \langle \phi_{M_{4s}} | H | \phi_{S_{3p}} \rangle$ and the energy difference $(E_{M_{4s}} - E_{S_{3p}})$:

$$\Delta E_{M_{4s},S_{3p}} \simeq -(H_{M_{4s},S_{3p}})^2/(E_{M_{4s}} - E_{S_{3p}})$$

Since, from section IIIA, the Zn(II) 4s orbital is lower in energy than the 4s orbital of Cu(I) (5.2 vs 2.2 eV), it is energetically more accessible for bonding. The smaller covalent bonding interaction found for Zn(II) as compared to Cu(I) must therefore be due to a smaller $H_{M_{4s},S_{3p}}$, which reflects the overlap between the ligand orbitals and metal 4s and 4p levels. Zn(II) has higher effective nuclear charge and smaller size than Cu(I). Consequently, its 4s orbital is highly contracted, resulting in less overlap and thus a weaker covalent bonding interaction. This observation is consistent with our previous study on the binding of CO to Zn(II) and Cu(I) surface sites[52] and with the smaller nephelauxetic effect on d-electron repulsion found for Zn(II) in section IIIA2, which indicates a greater orbital contraction of the Zn(II) ion in the oxide lattice.

(52) Lin, J.; Jones, P.; Guckert, J.; Solomon, E. I. *J. Am. Chem. Soc.* **1991**, *113*, 8312.

Coordination of the HS^- ligand to a metal ion results in mixing of metal 4s and 4p character into the HS^- bonding orbitals with the electron density being redistributed from the S–H bond.[42] The stronger Cu(I)–SH^- interaction should remove more charge from the S–H molecular orbital, weakening the S–H bond and activating it toward further deprotonation. Complete deprotonation therefore occurs more easily on the Cu_2O surface at low temperature and low coverages. Alternatively, complete deprotonation of H_2S is observed on the ZnO surfaces at room temperature but not at 140 K, implying that there exists a higher activation barrier for the deprotonation of the surface-bound HS^-, related to the weaker Zn(II)–SH^- interaction and thus stronger S–H bond. Accordingly, the strength of the metal–sulfur covalent bonding interaction is closely related to the catalytic sensitivity to sulfur poisoning.

In summary, $Cu_2O(111)$ is found to react with H_2S more strongly than ZnO(0001), which is parallel to the known catalytic chemistry: it adsorbs H_2S more easily with a higher sticking probability, decomposes H_2S to form sulfide at lower temperature (140 K vs room temperature for ZnO), and binds HS^- more strongly. The higher affinity of Cu(I) to H_2S and its deprotonated products is attributed to reduced orbital contraction and thus greater covalent bonding as compared to Zn(II). The stronger Cu(I)–SH^- bonding interaction weakens the S–H bond and thus lowers the activation barrier for formation of sulfide, resulting in more facile dissociative adsorption of H_2S on Cu(I) than Zn(II). Selective deposition of sulfide adsorbate on the Cu(I) surface site would block the catalytic active center, leading to more effective sulfur poisoning of Cu-promoted ZnO catalysts.

Acknowledgment. We thank Prof. C. Schwab, Universite Louis Pasteur, France, for providing the Cu_2O single crystal used in this study. This work is supported by the NSF-MRL Program through the Center for Materials Research at Stanford University. Support for the work done at Stanford Synchrotron Radiation Laboratory, which is operated by the Department of Energy, Division of Chemical Sciences, is gratefully acknowledged.